

## Intrachain charge generation and recombination in alkoxy-substituted poly-(*p*-phenylenevinylene) films

S. Stagira, M. Nisoli, G. Lanzani, and S. De Silvestri  
*INFN–Dipartimento di Fisica, Politecnico di Milano, Milano, Italy*

T. Cassano and R. Tommasi  
*INFN–Dipartimento di Fisica, Università degli Studi di Bari, Bari, Italy*

F. Babudri, G. M. Farinola, and F. Naso  
*Centro CNR di Studio sulle Metodologie Innovative di Sintesi Organiche, Dipartimento di Chimica, Università degli Studi di Bari, Bari, Italy*

(Received 25 May 2001; published 30 October 2001)

The role of intrachain processes in ultrafast charge photogeneration has been investigated in solid state for two dialkoxy PPV derivatives, characterized by an open-chain and a closed-chain substitution, respectively. In spite of the different strength of the intermolecular interaction induced by the chemical structure of substituents, similar relaxation dynamics are observed in the first few ps. Two main relaxation pathways are individuated. Upon excitation, single-photon absorption processes generate singlet excitons, whose relaxation dynamics is initially governed by intrachain diffusion. Two-step absorption processes are responsible for generation of high-energy excited states, which decay towards intrachain charge-transfer states on a time scale faster than our temporal resolution. Ultrafast charge recombination is then observed in the first hundreds of fs.

DOI: 10.1103/PhysRevB.64.205205

PACS number(s): 78.47.+p, 78.66.Qn, 72.80.Le, 72.20.Jv

### I. INTRODUCTION

The availability of highly fluorescent conjugated polymers has opened the way to a large number of applications in optoelectronics, including light-emitting diodes<sup>1,2</sup> optically-pumped lasers,<sup>3–5</sup> transistors,<sup>6,7</sup> and photocells.<sup>8</sup> The improvement of polymeric devices and the development of new optoelectronic components are based onto the understanding of photophysics in such materials. Among the numerous issues addressed in this field, particular attention has been directed towards the photogeneration of charged species in conjugated polymers. According to some authors, photocarriers are directly generated upon photoexcitation<sup>9,10</sup> with the same quantum efficiency at low or high pump energy; the carrier recombination rate appears to depend strongly on pump energy and interchain distance. For strong interchain interaction, charge separation is more likely to take place, resulting in a longer recombination time. A different model of charge photogeneration<sup>11</sup> assumes that excitons are the only primary photoexcitation initially created by the pump pulse; charged species are secondary excitations generated *via* intensity-dependent processes or dissociation. Such generation channels are individuated in Auger processes involving exciton–exciton annihilation, in the decay of biexcitons generated by two-photon absorption or in dissociation mediated by electron-trapping sites. Both the two models assign a central role to interchain interaction. In this framework the contribution of intrachain processes to carrier dynamics is disregarded or is considered of minor importance with respect to interchain processes. Nevertheless this approach leaves some issues open, concerning: (a) the role of intrachain processes in carrier generation and (b) the electron-hole dynamics before the occurrence of charge separation on adjacent chains. Answers to these questions need a detailed

description of the excitation dynamics occurring in the investigated material, in order to distinguish between charged and neutral species and to recognize the relationship between them. From this point of view, poly-phenylenevinylene (PPV) is one of the most studied materials among conjugated polymers. The investigation of photoexcitation dynamics in PPV has been performed via ordinary pump–probe spectroscopy<sup>11–14</sup> polarization anisotropy measurement<sup>15</sup> three-beam transient spectroscopy<sup>16,17</sup> infrared active vibrational mode (IRAV) spectroscopy<sup>9,10</sup> fluorescence decay measurements<sup>18,19</sup> and fluorescence line-narrowing characterization.<sup>20</sup> Charge-transfer processes in PPV have been studied both theoretically<sup>21</sup> and experimentally through photocurrent spectra<sup>22</sup> and pump–probe measurement.<sup>23,24</sup> Owing to its detailed characterization, we have chosen the PPV structure as a test material, with the aim of single out the role of intrachain processes in the photocarrier dynamics of conjugated polymers. For this purpose we present the measurements of transient transmission change ( $\Delta T/T$ ) in two PPV derivatives. The first one (DMB–PPV) has an open chain substitution; the second derivative (BDA–PPV) has a closed chain substitution. The chemical structure of the substituents is tailored to give a different strength of the interchain interaction for the two polymers in the solid state. The inhibition of intermolecular processes induced by the closed chain substitution, allows to attribute the relaxation dynamics in BDA–PPV mainly to intrachain processes. Nevertheless the strong similarity observed in the initial decay dynamics of the two polymers, claims for initial intrachain evolution also in DMB–PPV. Analysis of  $\Delta T/T$  measurements has revealed two different relaxation pathways in both the polymers: the first one is associated to exciton decay, whereas the second process is intensity dependent and is ascribed to charge photogeneration and recombination. On the

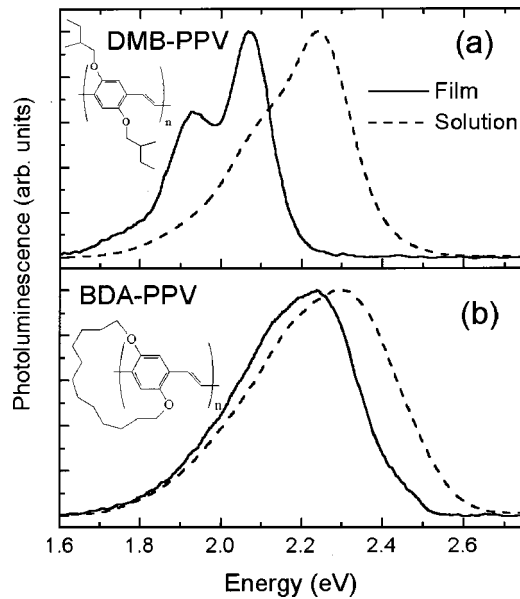


FIG. 1. (a) Photoluminescence spectra of DMB-PPV in film (solid line) and solution (dashed line). (b) Photoluminescence spectra of BDA-PPV in film (solid line) and solution (dashed line); the chemical structures of the two polymers are shown as inset.

basis of experimental results, we argue that charge generation take place through the excitation of an even-symmetry high-energy state, which decays into a charge transfer (CT) state. On-chain recombination of the CT state occurs on the time scale of hundreds of fs.

## II. EXPERIMENT

Two alkoxy-substituted PPV have been synthesized, namely poly[2,5-bis(2-methylbutoxy)-1,4-phenylenevinylene] (DMB-PPV) and poly[2,15-dioxabicyclo[14.2.2]icosal(19),16(20),17-trien-17,19-ylenevinylene] (BDA-PPV), which were prepared *via* the Stille cross-coupling reaction.<sup>25</sup> They have similar degree of polymerization and polydispersity indexes.<sup>26</sup> The chemical structure of DMB-PPV is reported in Fig. 1(a) as inset. The BDA-PPV has a closed chain substitution consisting of a 2,5-O-(CH<sub>2</sub>)<sub>12</sub>-O bridge, as shown in the inset of Fig. 1(b). Thin films were prepared by spin coating the polymer solutions onto a fused silica substrate, obtaining a thickness of  $\sim 300$  nm. The cw photoluminescence (PL) spectrum of DMB-PPV, displayed in Fig. 1(a), shows a pronounced redshift passing from the solution to the film. This behavior is ascribed to strong interchain interactions in the solid state. A small shift is observed in the cw PL spectrum of BDA-PPV, as shown in Fig. 1(b). We ascribe this difference to the reduction of interchain interaction induced by the closed chain with respect to the open chain substitution. This assumption is also supported by PL efficiency measurements; the ratio,  $\rho$ , between efficiencies in film and in solution is higher in BDA-PPV<sup>26</sup> ( $\rho = 0.55-0.88$ ) with respect to DMB-PPV ( $\rho \sim 0.29$ ).

Measurements of transient transmission change ( $\Delta T/T$ ) were performed using a conventional pump-probe configuration. The samples were kept in vacuum at room tempera-

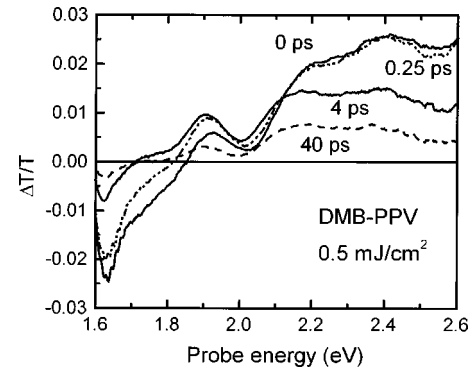


FIG. 2. Transient transmission change ( $\Delta T/T$ ) spectra in DMB-PPV for different pump-probe delays, measured at a pump fluence of  $0.5 \text{ mJ/cm}^2$ .

ture. The laser system, which has been described elsewhere,<sup>27</sup> consists of a Ti:sapphire laser with chirped-pulse amplification, which provides 150-fs pulses at 780 nm (1.59 eV), with energy up to  $750 \mu\text{J}$  at 1-kHz repetition rate. The white-light supercontinuum, ranging from 1.6 to 2.7 eV, generated focusing a portion of the laser beam in a thin sapphire plate, was used as a probe; the second harmonic (3.18 eV) of the laser pulses, generated in a 1-mm-thick LiB<sub>3</sub>O<sub>5</sub> crystal, was used to pump the investigated samples. Pump pulse duration (180 fs) was measured by self-diffraction technique.  $\Delta T/T$  measurements were performed in both spectral and temporal domains. It is worth noting that the pump photon energy used in our experiments is well above the absorption edge of PPV (which is around  $2.2 \text{ eV}$ )<sup>26</sup>.

## III. RESULTS

### A. Ultrafast relaxation dynamics in DMB-PPV

Figure 2 shows the  $\Delta T/T$  spectra measured in DMB-PPV for different pump-probe delays at an excitation fluence of  $0.5 \text{ mJ/cm}^2$ . Three positive bands are observed at 1.9, 2.2, and 2.4 eV. From a comparison with fluorescence and absorption spectra,<sup>26</sup> we can ascribe the first band to stimulated emission (SE) from the 0-1 replica of the  $1B_u \rightarrow 1A_g$  excitonic transition and the third band to photoinduced bleaching (PB). The band at 2.2 eV is a superposition of PB and SE from the 0-0 replica of the  $1B_u \rightarrow 1A_g$  transition. A negative band is observed around 1.65 eV; according to the literature, this band is mainly ascribed to photoinduced absorption (PA) from the  $1B_u \rightarrow kA_g$  transition.<sup>16</sup> The blue tail of a second PA band,<sup>17</sup> peaking around 1.1 eV, is also present in this region. This contribution to the absorption comes from the  $1B_u \rightarrow mA_g$  transition, occurring in very short conjugated segments of the polymer chain. Following the evolution of the  $\Delta T/T$  spectra, we observe a similar decay of the PA and PB bands. The SE band at 1.9 eV initially shows a formation, followed by a decay, slower than that observed in other spectral regions. Both SE and PB bands present a spectral relaxation, which is attributed to exciton diffusion towards longer conjugated segments.<sup>17,18</sup> We also observe a relaxation of the isosbestic point around 1.8 eV (corresponding to  $\Delta T/T = 0$ ). Figure 3 shows the  $\Delta T/T$  spectra measured in DMB-PPV at

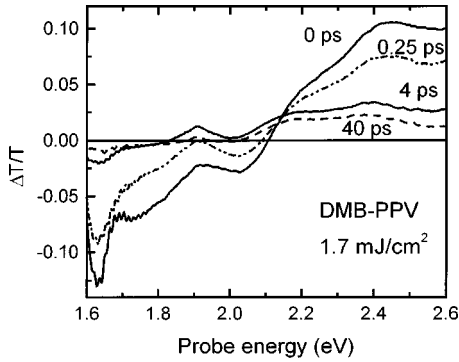


FIG. 3. Transient transmission change ( $\Delta T/T$ ) spectra in DMB-PPV for different pump-probe delays, measured at a pump fluence of  $1.7 \text{ mJ/cm}^2$ .

a higher excitation fluence ( $1.7 \text{ mJ/cm}^2$ ). The PA and PB bands measured at lower pump fluences are still present; a faster decay is observed in both the two spectral regions. The band at  $1.9 \text{ eV}$  shows a different behavior from the previous case: a strong PA appears at early time, turning into SE after  $250 \text{ fs}$ . This difference with respect to the spectral shape reported in Fig. 2 is an indication of a strong intensity-dependent process acting in the sample.

The ultrafast relaxation dynamics in DMB-PPV was also characterized in the temporal domain. Figure 4 shows the normalized pump-probe traces, measured at different probe energies ( $1.65$ ,  $1.91$ , and  $2.38 \text{ eV}$ ), for a pump fluence of  $0.5 \text{ mJ/cm}^2$ . The observed dynamics cannot be described in terms of single exponential decay. In order to single out the contributions coming from different processes, we have performed a time-constant analysis. Measurements at  $1.65 \text{ eV}$  (PA region) and at  $2.38 \text{ eV}$  (PB region) present a fast rise, limited by the pulse duration. Fittings show similar initial decay, characterized by a fast relaxation with a time constant  $\tau_1 \cong 270\text{--}300 \text{ fs}$ , followed by a slower decay, which can be fitted with two exponential components with time constants  $\tau_2 \cong 1.2 \text{ ps}$  and  $\tau_3 \cong 8 \text{ ps}$ ; the decay at  $1.65 \text{ eV}$  shows a higher weight of the  $\tau_1$  component. The analysis of the pump-probe trace at  $1.91 \text{ eV}$  reveals that the formation time of SE equals the fast decay time  $\tau_1$  of PA and PB. The initial decay of SE can be fitted by an exponential component with

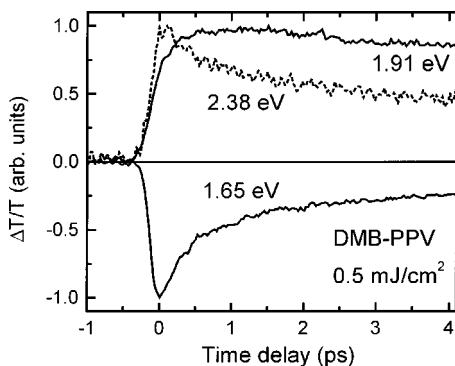


FIG. 4. Normalized pump-probe traces measured in DMB-PPV at probe energies of  $2.38 \text{ eV}$  (PB),  $1.91 \text{ eV}$  (SE), and  $1.65 \text{ eV}$  (PA) for an excitation fluence of  $0.5 \text{ mJ/cm}^2$ .

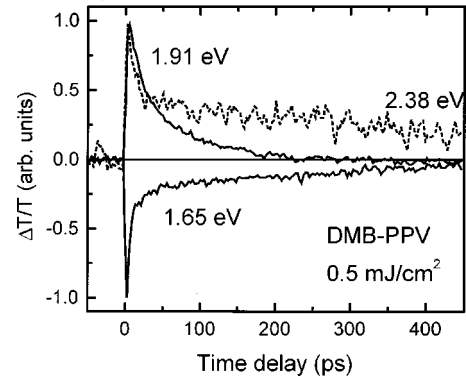


FIG. 5. Normalized pump-probe traces in DMB-PPV at probe energies of  $2.38 \text{ eV}$  (PB),  $1.91 \text{ eV}$  (SE), and  $1.65 \text{ eV}$  (PA), measured on a long time scale at an excitation fluence of  $0.5 \text{ mJ/cm}^2$ .

time constant corresponding to  $\tau_3$ . The lack of the  $\tau_2$  component accounts for the slower decay of SE with respect to the PA band, as observed in  $\Delta T/T$  spectra. On a longer time scale the PA at  $1.65 \text{ eV}$  decays according to an exponential law, with a time constant  $\tau_{\text{ex}} \cong 250 \text{ ps}$ , as shown in Fig. 5. Numerical fittings show that the measurement at  $1.91 \text{ eV}$  (SE region) can be modeled as the overlap of a long-lived absorption and an exponential decay with time constant  $\tau_{\text{ex}}$ . We relate  $\tau_{\text{ex}}$  to the exciton lifetime, in agreement with values reported in literature.<sup>16</sup> The long-lived absorption observed in the SE region could be due to polarons generated by interchain charge transfer.<sup>11</sup> Note that the PB signal at  $2.38 \text{ eV}$  presents correspondingly a plateau, thus indicating a not completed recovery of ground state. In order to understand the role of nonlinear effects on the relaxation dynamics, we have also performed pump-probe measurements at  $1.65$  and  $1.91 \text{ eV}$  for different pump fluences. The experimental results corresponding to  $1.91 \text{ eV}$  are reported in Fig. 6. One can see that, upon increasing the excitation fluence, a fast absorption signal develops, followed by gain formation. The risetime of this nonlinear absorption ( $\text{PA}_{\text{NL}}$ ) cannot be

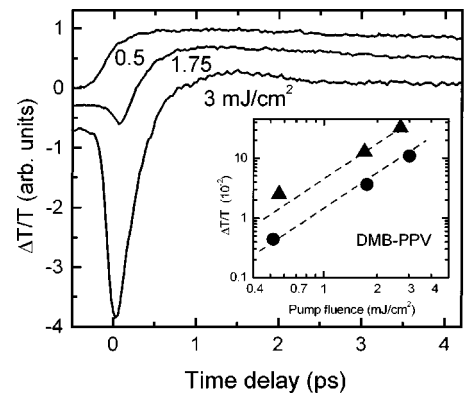


FIG. 6. Normalized pump-probe signal measured in DMB-PPV at a probe energy of  $1.91 \text{ eV}$  (SE) for different excitation fluences; the traces are displaced for readability. Inset: amplitude of absorption at  $1.91 \text{ eV}$  (filled dots) and at  $1.65 \text{ eV}$  (filled triangles) as a function of pump fluence; dashed lines report square dependence on fluence; errors are within symbol dimensions.

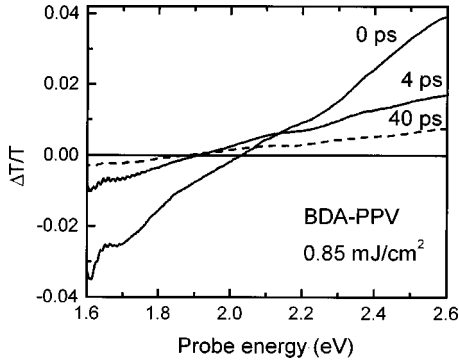


FIG. 7. Transient transmission change ( $\Delta T/T$ ) spectra in BDA-PPV for different pump-probe delays, measured at a pump fluence of  $0.85 \text{ mJ/cm}^2$ .

resolved with our temporal resolution. The decay of  $\text{PA}_{\text{NL}}$  is very fast, with a time constant equal to  $\tau_1$ .

### B. Ultrafast relaxation dynamics in BDA-PPV

Figure 7 shows the  $\Delta T/T$  spectra measured in BDA-PPV for different pump-probe delays at an excitation fluence of  $0.85 \text{ mJ/cm}^2$ . In spite of the conjugated structure similar to DMB-PPV, BDA-PPV shows some peculiar characteristics. A PA band is still observed around 1.6 eV, extending up to 2 eV (at zero time delay); thus we assign it again to photoinduced absorption (PA) from the excitonic transitions. A positive band extends from 2 to 2.7 eV; from a comparison with fluorescence and absorption spectra,<sup>26</sup> we ascribe it to overlap of photobleaching and stimulated emission. A detailed analysis of the spectra at long pump-probe delays, allows to recognize two small shoulders around 2.1 and 2.3 eV, which are assigned to SE from the 0-1 and 0-0 replica of excitonic transition, respectively.<sup>26</sup> Following the evolution of the  $\Delta T/T$  spectra, we observe a similar decay of the PA and PB bands. A spectral relaxation of the isosbestic point around 2 eV is observed; we ascribe it to the presence of exciton diffusion towards longer conjugated segments and to decay of different species affecting this spectral region. In order to investigate the role of nonlinear processes, pump-probe measurements were also performed at higher pump intensity. Figure 8 shows  $\Delta T/T$  spectra recorded at zero pump-probe delay for different pump fluences. In spite of the featureless structure of the spectra, occurrence of nonlinear effects is evidenced by the blue shift of the isosbestic point as fluence is increased.

The ultrafast relaxation dynamics in BDA-PPV was also characterized in the temporal domain. Figure 9 shows the normalized pump-probe traces, measured at different probe energies, at a pump fluence of  $0.8 \text{ mJ/cm}^2$ . As previously seen for DMB-PPV, the observed dynamics cannot be described in terms of a single exponential decay. A time constant analysis reveals a slower relaxation dynamics with respect to DMB-PPV. Numerical fits performed on measurements at 1.68 eV show a PA formation with a time constant  $\tau_f \approx 100 \text{ fs}$ , followed by an initial decay, which can be fitted with three exponential components with time constants  $\tau_1 \approx 500 \text{ fs}$ ,  $\tau_{\text{II}} \approx 2 \text{ ps}$ , and  $\tau_{\text{III}} \approx 20 \text{ ps}$ . The PB dynam-

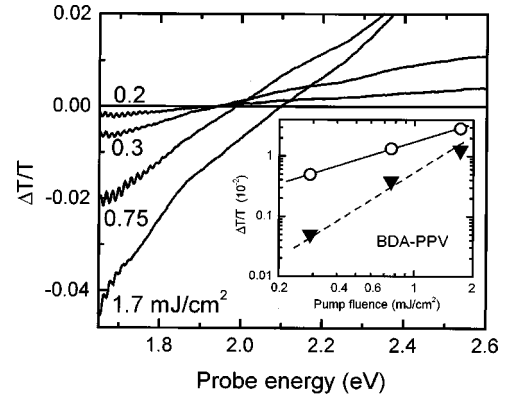


FIG. 8. Transient transmission change ( $\Delta T/T$ ) spectra in BDA-PPV for pump-probe delay of 0 ps, measured at different pump fluences. Inset: amplitude of nonlinear absorption at  $\sim 1.9 \text{ eV}$  (filled triangles) as a function of pump fluence; empty dots show absorption amplitude at 1.65 eV after subtraction of nonlinear contribution; solid (dashed) line reports linear (square) dependence on fluence; errors are within symbol dimensions.

ics at 2.70 eV presents a very fast initial relaxation, characterized by a combination of time constants  $\tau_f$  and  $\tau_1$  followed by a slower decay, which can be fitted with two exponential components with time constants  $\tau_{\text{II}}$  and  $\tau_{\text{III}}$ . A very different behavior is measured in the SE region at 2.25 eV, where initially we observe gain formation with a time constant corresponding to  $\tau_1$ . The initial gain decay is characterized uniquely by an exponential component with time constant  $\tau_{\text{III}}$ . Figure 10 reports the pump-probe traces measured at different probe energies on a longer time scale. Measurements present an exponential decay with a time constant  $\tau = 230 \text{ ps} \approx \tau_{\text{ex}}$ , thus similar to the value determined for DMB-PPV; this component is ascribed again to exciton lifetime.

## IV. DISCUSSION

The experimental results exposed previously show that the relaxation dynamics is substantially similar in the two PPV derivatives we considered. The differences between

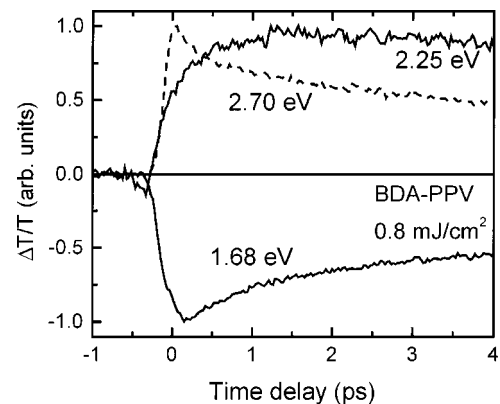


FIG. 9. Normalized pump-probe traces measured in BDA-PPV at probe energies of 2.70 eV (PB), 2.25 eV (SE), and 1.68 eV (PA) for an excitation fluence of  $0.8 \text{ mJ/cm}^2$ .



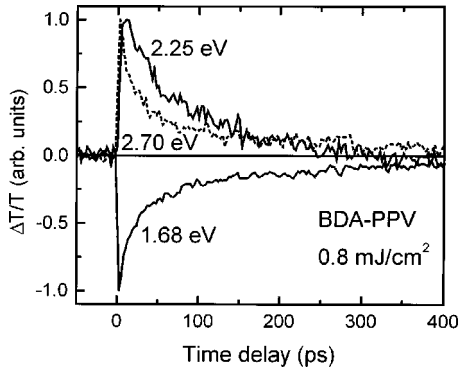


FIG. 10. Normalized pump-probe traces in BDA-PPV at probe energies of 2.70 eV (PB), 2.25 eV (SE), and 1.68 eV (PA) measured on a long time scale at an excitation fluence of 0.8 mJ/cm<sup>2</sup>.

time constants determined by numerical fitting, can be explained in terms of small influence of the chain substitution on the physical properties of the polymer. This is also evidenced by the small difference in the spectral shapes of photoluminescence detected in solution, as shown in Fig. 1. It is worth noting that the longest observed time constant which is related to the exciton lifetime  $\tau_{ex}$ , is essentially the same in the two materials and is interpreted as a signature of the common backbone structure. As mentioned previously, the closed-chain substitution allows to reduce the interchain interaction with respect to the open-chain one. On the basis of this consideration, we assume that the initial relaxation dynamics observed in BDA-PPV is associated to intrachain evolution of excited species. Owing to the similarity between dynamics in the two derivatives, we infer that there is a predominant intrachain contribution to initial dynamics also in DMB-PPV, in spite of the stronger intermolecular interaction observed in this material. In the following we address in more detail the contribution of linear and nonlinear processes observed in the two polymers in the first few ps and we present an interpretation of the experimental results.

### A. Linear processes

As mentioned before, the decay of PA is substantially different from that of SE in both the two polymers: PA in DMB-PPV presents a fast rise, limited by pulse duration, followed by a decay, fitted with three exponential components (time constants  $\tau_1$ ,  $\tau_2$ , and  $\tau_3$ ); SE presents a formation time  $\tau_1$  followed by a decay with time constant  $\tau_3$ . We observe the same behavior in BDA-PPV, except for the different values of time constants ( $\tau_1$ ,  $\tau_{II}$ , and  $\tau_{III}$ ). The lack of decay component with time constant  $\tau_2(\tau_{II})$  in SE dynamics can be explained in terms of diffusion processes. Upon photoexcitation, short conjugation segments are predominantly excited owing to the high pump photon energy, as shown in the scheme presented in Fig. 11(a). Following photoexcitation, ultrafast exciton thermalization occurs (indicated as  $T$  in the figure). Then excitation diffuses towards longer conjugation segments (process indicated as  $Df$ ), giving rise to spectral relaxation in pump-probe measurements. The effects of diffusion on temporal dynamics strongly depend on probe energy. The decay of pump-probe signal near a band peak is

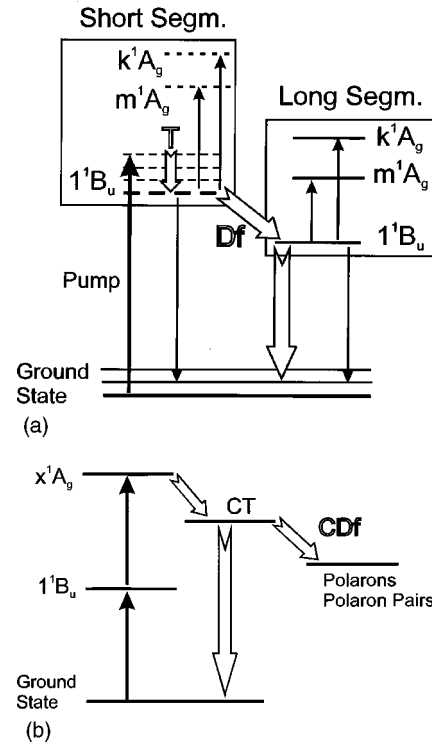


FIG. 11. (a) Energy level scheme for one-photon excitation process:  $T$ , exciton thermalization;  $Df$ , exciton diffusion; solid arrows, transition contributing to pump-probe signal; empty arrows, relaxation pathways. (b) Energy level scheme for two-step excitation process;  $Cdf$ : interchain charge diffusion.

slightly affected by diffusion; on the contrary, pump-probe measurements are strongly affected by diffusion on band tails. Measurements in the SE region were performed near the gain peak in both the two material; for this reason diffusion has small influence on these temporal decays. On the other hand, the blue tail of the  $1B_u \rightarrow mA_g$  band affects measurements in the PA region for both the two polymers. Thus temporal decay of PA is strongly affected by diffusion.<sup>17</sup> On this basis, we ascribe the time constant  $\tau_2(\tau_{II})$ , observed only in the PA decay, to exciton diffusion. This assumption is consistent with the spectral relaxation dynamics clearly observed in DMB-PPV (see Fig. 2). The process is less evident in BDA-PPV spectra, owing to their featureless structure.

Since interchain interaction is inhibited in BDA-PPV, we assume that exciton diffusion is predominantly an intrachain process in this polymer. Moreover the similarity between values of time constants  $\tau_2$  and  $\tau_{II}$ , is an indirect evidence that intrachain diffusion initially occurs also in DMB-PPV, in spite of the stronger intermolecular interaction.

The main difference between the dynamics in the two polymer is the occurrence of PA formation in BDA-PPV with time constant  $\tau_f$ . We speculate that this behavior could be related to exciton thermalization. The lack of similar observation in the PA dynamics measured in DMB-PPV, may be due to more efficient energy dissipation with respect to BDA-PPV, thus providing a faster relaxation, not observable within our temporal resolution.

### B. Nonlinear processes

Measurements resolved both in temporal and spectral domain have shown the occurrence of intensity-dependent phenomena in the two polymers. As a matter of fact, the SE and PA regions in DMB-PPV are affected by nonlinear absorption (see Figs. 3 and 6). Numerical fittings have evidenced that the time constant observed in the SE formation ( $\tau_1$ ) is identical to the initial time constant in PA decay. We interpret the experimental results assuming that the absorption from a nonlinear species ( $PA_{NL}$ ) overlaps, at short pump-probe delays, the spectral region of SE and PA (1.6–2.1 eV). According to this model, both the SE formation at 1.9 eV and the initial PA decay at 1.6 eV are explained as the decay of  $PA_{NL}$  with a time constant equal to  $\tau_1$ . To enforce this picture, we report in the inset of Fig. 6 the amplitude of  $PA_{NL}$  at 1.91 eV as a function of pump fluence (filled dots);  $PA_{NL}$  was extracted by numerical fits from pump-probe traces at this probe energy. One can see that  $PA_{NL}$  grows according to a square law, reported as dashed line. To prove that nonlinear absorption occurs also in the PA region, we display in the same plot the  $\Delta T/T$  peaks at 1.65 eV as a function of pump fluence (filled triangles). The nonlinear dependence on intensity is clear even in this case. It is worth noting that the risetime of pump-probe traces at 1.65 eV is always limited by laser pulse duration; same observation can be done when considering the risetime of the absorption at 1.91 eV (see traces at high pump fluence in Fig. 6). According to the experimental results, the  $PA_{NL}$  signal appears instantaneously; thus the nonlinear species responsible for this signal must be generated within the pump pulse.

The occurrence of nonlinear absorption is also observed in BDA-PPV, as evidenced in Fig. 8 by the blueshift of the isosbestic point, at zero pump-probe delay, as fluence increases. Assuming the crossing point at lowest pump as a reference (corresponding to  $\sim 1.9$  eV), we have extracted the  $\Delta T/T$  values at this probe energy as a function of pump fluence; the experimental results are reported in the inset of Fig. 8 as filled triangles. The pump-probe signal grows according to a square law, as evidenced by the dashed line. We argue that this behavior is again ascribed to a nonlinear species which absorbs from 1.6 to 2.2 eV. As further confirmation of this assumption, we show in the same inset the  $\Delta T/T$  signal at 1.65 eV after subtraction of the contribution measured at 1.9 eV (empty dots). This quantity shows a linear dependence on the pump fluence (as indicated by the solid line), so we argue that this is the absorption component induced by excitons.

Some detailed considerations must be reserved to the dynamics of the intensity-dependent species observed in both the two polymers. As previously mentioned, the initial fast relaxation measured in the PA region is characterized by the same time constant observed in SE formation. This result is interpreted assuming that a photogenerated species, different from singlet exciton, absorbs in a broad spectral region ranging from 1.6 to 2.1 eV, overlapping both PA and SE excitonic bands. The presence of a nonexcitonic species, responsible for competition between SE and PA, is a well-known finding in PPV studies, as testified by both early<sup>21,23,24</sup> and more

recent works.<sup>11</sup> Nevertheless the assignment of such species is still controversial. According to the literature, this could be identified with excimers, polaron pairs or polarons generated via interchain charge transfer. Excimer is an excited dimer that is dissociative in the ground state.<sup>28</sup> The formation of this species depends dramatically on intermolecular packing<sup>29</sup> and is more likely to take place in materials with strong interchain interaction. According to theoretical calculation<sup>30</sup> excimer lifetime should be longer than exciton lifetime; moreover excimer density should be linearly dependent on pump intensity and should have a noninstantaneous formation dynamics. All these considerations are in disagreement with our findings: according to measurements, the absorption  $PA_{NL}$  induced by the considered species appears within the pump pulse and has a quadratic dependence on excitation density; this absorption is detected also in BDA-PPV, which shows low intermolecular interaction; finally the decay of  $PA_{NL}$  is very fast, so it is not compatible with excimer lifetime. These considerations allow to discard the hypothesis based onto excimers generation.

On the basis of similar considerations, the assignment of the investigated species to polarons or polaron pairs generated by interchain charge transfer is unsatisfactorily, because we should observe a lack of  $PA_{NL}$  in BDA-PPV. This consideration comes from the assumption that interchain charge transfer requires a strong intermolecular interaction, that is inhibited in BDA-PPV. Moreover the very fast relaxation dynamics is not compatible with long-distance charge separation, because we would expect in this case a very long decay time constant associated with recombination processes.<sup>11</sup> It is worth noting that the nonlinear phenomena observed by Krabeel and co-workers in phenylene-based conjugated polymers, which are assigned to positively charged polarons, show the opposite dynamics we measured: in  $\Delta T/T$  spectra they observe a blueshift of isosbestic point as time advances, which is interpreted as generation of polarons by diffusion of charges towards adjacent chain, resulting in growing of absorption. On the contrary, we observe a fast redshift of isosbestic point in both the two derivative (see Fig. 2, 3, and 7), thus corresponding to a fast decay of absorption from the nonlinear species.

According to the previous considerations, we ascribe the  $PA_{NL}$  signal to the generation and subsequent fast decay of intrachain charged species by means of an intensity-dependent mechanisms. Figure 11(b) shows the scheme proposed for this nonlinear process: a high-energy even-symmetry state (indicated as  $x^1A_g$ ) is excited by two-step photon absorption; such process could either occur by sequential absorption through the intermediate excitation of the  $1^1B_u$  state or directly by two-photon absorption. The first mechanism appears more likely to occur; nevertheless it's worth noting that in both cases the high energy state would be generated within the pump pulse. Following excitation, the  $x^1A_g$  state quickly relaxes to a charge-transfer state [indicated as CT in Fig. 11(b)]. The term “charge transfer state” is considered here as an excited state with a finite probability of finding electron and hole separated by few phenylene rings on the chain. We ascribe the transient absorption  $PA_{NL}$  in the spectral region overlapping the PA and SE bands, to

this CT state. The observed decay of the  $\text{PA}_{\text{NL}}$  signal is then interpreted as a very fast geminate recombination of the charged pair in the CT state. Such recombination accounts also for the fast initial recovering of the bleaching signal. Our assumption is supported by theoretical models and measurements of photocurrent spectra in PPV,<sup>22</sup> which show that CT states can be excited at 5.5 and 7 eV, corresponding to the so called III and V absorption bands of PPV. In our experimental conditions, the CT state responsible for the III band can be reached by two-step photon excitation (which corresponds to a total absorbed energy of 6.4 eV) followed by energy relaxation. The difference between the absorbed energy and the energy of the CT state (which amounts to  $\sim 0.9$  eV) could be dissipated through phonon emission in the ultrafast decay from  $x^1A_g$  to CT; nevertheless, a certain amount of the excess energy could also be dissipated through the fast thermalization of the  $1^1B_u$  state, before the absorption of the second photon. Both the two mechanisms are possible; anyway the risetime of the  $\text{PA}_{\text{NL}}$  signal is limited by pulse duration, so we infer that dissipation of the excess energy must take place on a time scale shorter than our temporal resolution. According to our model, following photoexcitation a considerable fraction of generated charges undergoes recombination; if the intermolecular interaction is sufficiently strong, the surviving pairs undergo separation and charge diffusion to neighboring polymer chains [process indicated as Cdf in Fig. 11(b)]; in this way a certain amount of polaron or polaron pairs is generated, depending on the strength of the intermolecular interaction. Such species contribute to long-lived absorption signal in the SE-PA spectral region of PPV.<sup>11</sup> A long-lived absorption is actually observed in DMB-PPV around 1.9 eV and correspondingly a long-lived bleaching is present at 2.38 eV (see Fig. 5), because in this polymer charge transfer among adjacent chains is more likely to take place. Smaller long-lived component of absorption and bleaching are observed in BDA-PPV (see Fig. 10), where charge transfer towards adjacent chains is inhibited. On the basis of this model, we assume that the closed chain substitution in BDA-PPV forces an almost complete recombination of the CT states generated at high pump intensity.

A justified question concerns the electron-hole recombination process. It is questionable whether the CT states recombine nonradiatively towards the ground state or towards an excitonic state. It is well known that electron-hole recombination in a polymeric LED gives rise to excitons, thus providing a source of light emission through singlet exciton radiative decay. Nevertheless the fast initial decay of the PB signal, observed in both polymers, indicates ground state recovery, in favor of the first hypothesis. If the CT state recom-

bination would lead to generation of an intermediate excited state, ground state recovery would not take place and the PB would be insensitive to the process; its decay would be slower with lack of the  $\tau_1(\tau_1)$  time constant. It must be pointed out that the CT state considered here is an intrachain species; thus the charged pair in this state undergoes geminate recombination. On the other hand, exciton generation in polymeric electrically pumped devices takes place from the recombination of interchain nongeminate pairs. Thus the strong difference between the two situations does not allow a stringent comparison of charge recombination processes.

## V. CONCLUSIONS

The ultrafast relaxation dynamics in two PPV derivatives has been investigated both in spectral and temporal domain. The first derivative has open chain substitution (DMB-PPV), which allows interchain interaction; the second derivative has closed chain substitution (BDA-PPV), which inhibits interchain interaction. The occurrence of linear and intensity-dependent processes were observed in both materials. We propose two photoexcitation mechanisms to explain our observations. Upon excitation, single-photon absorption processes generate singlet excitons, whose relaxation dynamics is then governed by intrachain diffusion in the first few ps. Two-step absorption processes are responsible for generation of high-energy even-symmetry excited states ( $x^1A_g$ ). These states decay towards intrachain charge-transfer states (CT) on a time scale faster than our temporal resolution. Ultrafast charge recombination is then observed in the first hundreds of fs. The strength of intermolecular interaction governs the probability of charge diffusion among adjacent chains before recombination has completed. Initial dynamics of the two above-cited relaxation mechanisms has small dependence on chain substitution, with a slower behavior in BDA-PPV. The occurrence of higher long-lived component in DMB-PPV, which is ascribed to polarons, is an indication that charge separation and diffusion is more probable for open-chain substitution.

## ACKNOWLEDGMENTS

The authors gratefully acknowledge L. Chiavarone and G. Scamarcio for their participation at the early stage of the experiment. This work was partially financially supported by Ministero dell'Università e della Ricerca Scientifica e Tecnologica, Rome (Project "Sintesi di materiali organici per applicazioni ottiche" L.488 19/12/92, Piano "Materiali Innovativi").

<sup>1</sup>J. Burroughes, D. D. C. Bradley, A. Brown, R. Marks, K. Machay, R. Friend, P. Burns, and A. Holmes, *Nature (London)* **347**, 539 (1990).

<sup>2</sup>D. Braun and A. Heeger, *Appl. Phys. Lett.* **58**, 1982 (1991).

<sup>3</sup>N. Tessler, G. J. Denton, and R. H. Friend, *Nature (London)* **382**, 695 (1996).

<sup>4</sup>S. Stagira, M. Zavelani-Rossi, M. Nisoli, S. De Silvestri, G. Lanzani, C. Zenz, P. Mataloni, and G. Leising, *Appl. Phys. Lett.* **73**, 2860 (1998).

<sup>5</sup>S. Frolov, M. Shkunov, Z. Vardeny, and K. Yoshino, *Phys. Rev. B* **56**, R4363 (1997).

<sup>6</sup>F. Garnier, R. Hailaoui, A. Yassar, and P. Srivastava, *Science* **265**,

- 1684 (1994).
- <sup>7</sup>D. Gundlach, Y. Lin, T. Jackson, and D. Schlom, *Appl. Phys. Lett.* **71**, 3853 (1997).
- <sup>8</sup>G. Yu, J. Gao, J. C. Hummelen, F. Wudl, and A. J. Heeger, *Science* **270**, 1789 (1995).
- <sup>9</sup>D. Moses, A. Dogariu, and A. J. Heeger, *Chem. Phys. Lett.* **316**, 356 (2000).
- <sup>10</sup>D. Moses, A. Dogariu, and A. J. Heeger, *Phys. Rev. B* **61**, 9373 (2000).
- <sup>11</sup>B. Kraabel, V. I. Klimov, R. Kohlman, S. Xu, H-L. Wang, and D. W. McBranch, *Phys. Rev. B* **61**, 8501 (2000).
- <sup>12</sup>J. M. Leng, S. Jeglinski, X. Wei, R. E. Benner, Z. V. Vardeny, F. Guo, and S. Mazumdar, *Phys. Rev. Lett.* **72**, 156 (1994).
- <sup>13</sup>H. S. Eom, S. C. Jeoung, D. Kim, J. I. Lee, H. K. Shim, C. M. Kim, C. S. Yoon, and K. S. Lim, *Appl. Phys. Lett.* **71**, 563 (1997).
- <sup>14</sup>G. J. Denton, N. Tessler, N. T. Harrison, and R. H. Friend, *Phys. Rev. Lett.* **78**, 733 (1997).
- <sup>15</sup>B. Kraabel and D. W. McBranch, *Chem. Phys. Lett.* **330**, 403 (2000).
- <sup>16</sup>S. V. Frolov, Z. Bao, M. Wohlgenannt, and Z. V. Vardeny, *Phys. Rev. Lett.* **85**, 2196 (2000).
- <sup>17</sup>S. V. Frolov, Z. Bao, M. Wohlgenannt, and Z. V. Vardeny, *Phys. Rev. B* (to be published).
- <sup>18</sup>R. Kersting, U. Lemmer, R. F. Mahrt, K. Leo, H. Kurz, H. Bässler, and E. O. Göbel, *Phys. Rev. Lett.* **70**, 3820 (1993).
- <sup>19</sup>G. R. Hayes, I. D. W. Samuel, and R. T. Phillips, *Phys. Rev. B* **56**, 3838 (1997).
- <sup>20</sup>S. V. Frolov, W. Gellermann, M. Ozaki, K. Yoshino, and Z. V. Vardeny, *Phys. Rev. Lett.* **78**, 729 (1997).
- <sup>21</sup>H. A. Mizes and E. M. Conwell, *Phys. Rev. B* **50**, 11243 (1994) (Rapid Communication).
- <sup>22</sup>A. Köhler, D. A. dos Santos, D. Beljonne, Z. Shuai, J.-L. Brédas, A. B. Holmes, A. Kraus, K. Müllen, and R. H. Friend, *Nature (London)* **392**, 903 (1998).
- <sup>23</sup>J. W. P. Hsu, M. Yan, T. M. Jedju, and L. J. Rothberg, *Phys. Rev. B* **49**, 712 (1994).
- <sup>24</sup>M. Yan, L. J. Rothberg, F. Papadimitrakopoulos, M. E. Galvin, and T. M. Miller, *Phys. Rev. Lett.* **72**, 1104 (1994).
- <sup>25</sup>F. Babudri, S. R. Cicco, L. Chiavarone, G. M. Farinola, L. C. Lopez, F. Naso, and G. Scamarcio, *J. Mater. Chem.* **10**, 1573 (2000).
- <sup>26</sup>L. Chiavarone, M. Di Terlizzi, G. Scamarcio, F. Babudri, G. M. Farinola, and F. Naso, *Appl. Phys. Lett.* **75**, 2053 (1999).
- <sup>27</sup>G. Cerullo, S. Stagira, M. Nisoli, S. De Silvestri, G. Lanzani, G. Kranzelbinder, W. Graupner, and G. Leising, *Phys. Rev. B* **57**, 12806 (1998).
- <sup>28</sup>J. Birks, *Photophysics of Aromatic Molecules* (Wiley-Interscience, London, 1970).
- <sup>29</sup>Hsin-Fei Meng, *Phys. Rev. B* **58**, 3888 (1998).
- <sup>30</sup>E. M. Conwell, *Phys. Rev. B* **57**, 14200 (1998).